Photoswitchable Compounds

DOI: 10.1002/anie.201107086

High-Contrast Reversible Fluorescence Photoswitching of Dye-Crosslinked Dendritic Nanoclusters in Living Vertebrates**

Yoonkyung Kim, Hye-youn Jung, Yun Hui Choe, Chaewoon Lee, Sung-Kyun Ko, Soonil Koun, Yohan Choi, Bong Hyun Chung, Byoung Chul Park, Tae-Lin Huh, Injae Shin, and Eunkyoung Kim*

Recent advances in fluorescence imaging have made this technique indispensable not only for in vitro investigations of cells and proteins, but also for in vivo imaging.[1] The sensitivity of in vivo fluorescence imaging, which is generally limited by autofluorescence, absorbance, light scattering, and penetration depth, has been improved significantly, for example, by employing switchable probes.[2] The utility of such probes mostly for diagnostic purposes in vivo, however, can be restricted by their low on–off contrast, irreversibility, poor delivery, and toxicity. In an effort to make fluorescence-imaging agents for in vivo applications, herein we prepared biocompatible dendritic nanoclusters that can repeatedly exhibit high on–off contrast inside the living zebrafish without any apparent toxicity. Specifically, a diarylethene[3] derivative, which interconverts between two isomeric forms by alternate irradiation with UV and visible light,[4] was used to crosslink dendrimers and to reversibly quench the fluorescence of a neighboring fluorophore through fluorescence resonance energy transfer (FRET).[5]

The synthesis of dendritic nanoclusters is illustrated in Scheme 1. Our primary concern in designing a reversible photoswitch was to achieve the maximal fluorescence contrast between the activated and quenched states while avoiding (or minimizing) self-quenching[1,2] of fluorescence that may occur when the fluorophores with highly extended π conjugation (e.g., cyanine 3 (Cy3)) are positioned in close proximity to each other. In fact, the active form of diarylethene (FRET acceptor) that can truly quench the fluorescence of Cy3 (FRET donor) is limited to the ring-closed isomer[3,5] (derived from the antiparallel conformation of the ring-open isomer), which constituted about 50 mol% of all diarylethene available after irradiating with UV light when monitored by ^{1}H NMR spectroscopy (see Figure S1 in the Supporting Information). Accordingly, sparse attachment of Cy3 at the fifth generation (G5) polyamidoamine (PAMAM) dendrimer[6] (ca. 5 nm[7] in diameter) was intended, while controlling the stoichiometry so that its molar content did not exceed 50% of the diarylethene attached to the dendrimer. Second, instead of using a dendrimer as the platform, dendrimers were oligomerized[8] to form a nanocluster (**3**) using the diarylethene **2**[9] as a crosslinker. By forming an oligomer, both intra- and inter-dendritic FRET within the same nanocluster can be achieved, and at the same time the fluorescence signal of Cy3 from a single molecular entity can be amplified (nanocluster vs. dendrimer). Moreover, rather than attaching diarylethene moieties to the surface of a preformed nanoparticle of similar dimensions, the formation of such a porous nanocluster was sought to better distribute the diarylethene and Cy3 throughout the nanostructure (both interior and exterior), leading to more efficient FRET. Third, to obtain a narrow size distribution of nanoclusters, and thus to exert more homogeneous biological effects, our dendritic nanoclusters were 1) synthesized according to a procedure to prepare size-controlled dendritic nanoclusters[8a] (similar reaction concentration and feed ratio) and 2) partially fractionated by size using preparative size-exclusion chromatography (SEC). The analysis of NMR integration and MALDI both indicated that approximately 1.9 diarylethene units were attached per dendrimer (Figures S5 and S9, Table S1 in the Supporting Information). Finally, the residual surface amino groups of dendritic nanocluster **5** were converted into a more biocompatible functionality in the final synthetic step by treating them with either 1) succinic anhydride to make an anionic surface with carboxylate groups (for **6**) or 2) the *N*-hydroxysuccinimide (NHS) ester of tetra(ethylene glycol) methyl ether (mTEG) to make a neutral surface (for **7**). Both surface modifications, as confirmed by measuring the zeta potential (Table S2 in the Supporting Information), yielded dendritic nanoclusters (ca. 20 nm) with

[*] Dr. Y. Kim, H.-y. Jung, Y. H. Choe, C. Lee, Y. Choi, Dr. B. H. Chung, Dr. B. C. Park
Korea Research Institute of Bioscience and Biotechnology
Daejeon, 305-806 (Korea)
E-mail: ykim@kribb.re.kr
S.-K. Ko, Prof. Dr. I. Shin
Department of Chemistry, Yonsei University, Seoul, 120-749 (Korea)
S. Koun, Prof. Dr. T.-L. Huh
School of Life Sciences and Biotechnology
Kyungpook National University, Daegu, 702-701 (Korea)
Prof. Dr. E. Kim
Department of Chemical and Biomolecular Engineering
Yonsei University, Seoul, 120-749 (Korea)

[**] We are grateful to Dr. Haijun Yao at the Mass Spectrometry Laboratory of the University of Illinois for collecting MALDI spectra of our dendrimer samples. We thank Drs. Kang Taek Lee and Sang Hwan Nam for the measurement of the photobleaching rate, Dr. Nyeon-Sik Eum, Chijung Yun, and Dr. Nam Woong Song for the assistance with the installation of optical equipments, and Prof. Dr. Joon Kim for allowing us to use the DeltaVision imaging system. This work was supported by the National Research Foundation of Korea (2010-0008056, 2010-0002205) funded by the Ministry of Education, Science and Technology and the KRIBB Research Initiative Program.

Supporting information for this article is available on the WWW under http://dx.doi.org/10.1002/anie.201107086.

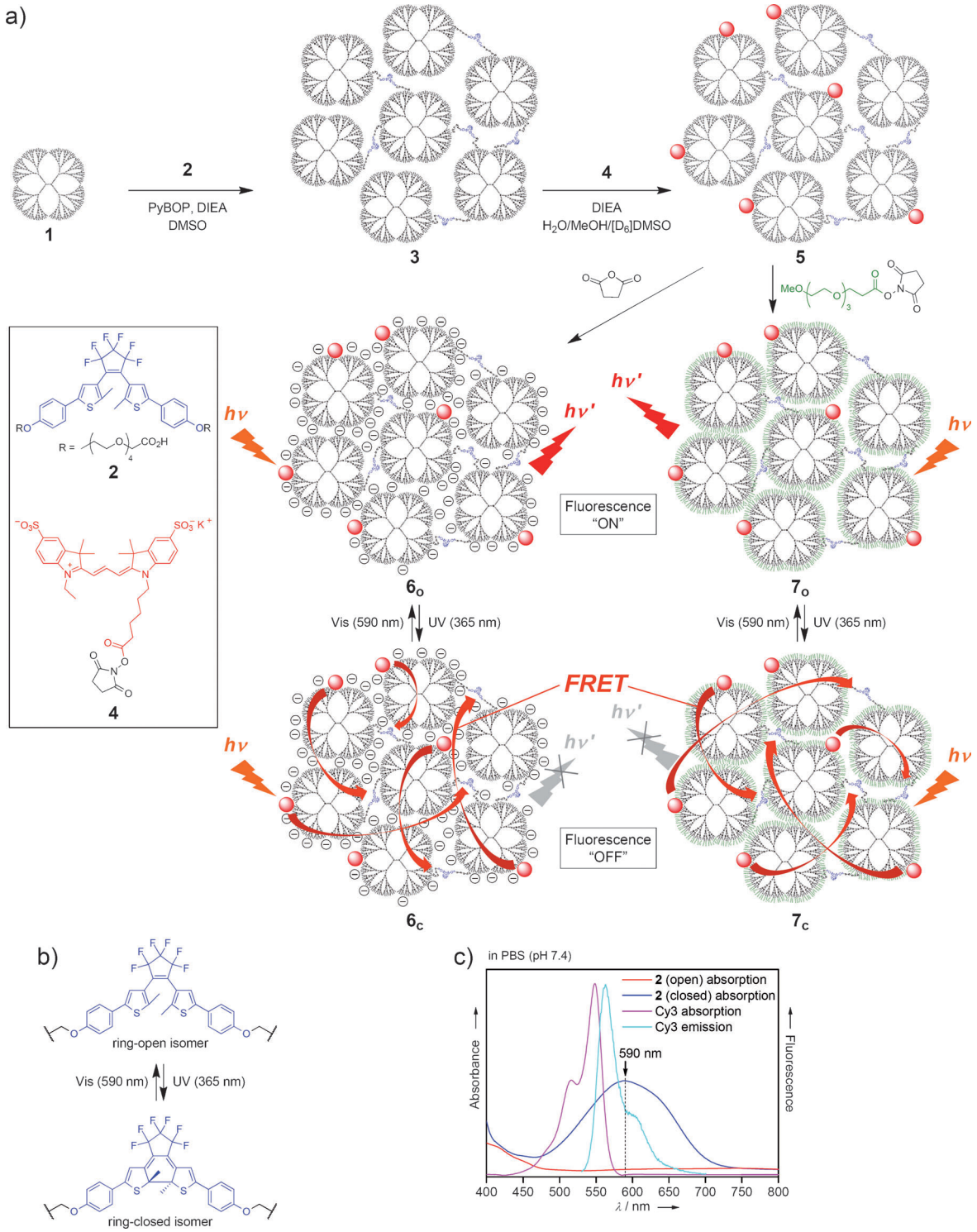

Scheme 1. a) Synthesis of dye-crosslinked dendritic nanoclusters. The subscripts "o" and "c" in the compound numbers of **6** and **7** denote the ring-open and ring-closed isomers of diarylethene derivatives, respectively. Red circles represent the Cy3 moieties as covalently attached to the surface of dendrimers. For solution samples, $h\nu = 510$ nm and $h\nu' = 566$ nm. PyBOP = (benzotriazol-1-yl-oxy)tripyrrolidinophosphonium hexafluorophosphate, DIEA = diisopropylethylamine, DMSO = dimethylsulfoxide. b) Switching between the ring-open and ring-closed isomers of diarylethene derivatives. c) UV/Vis absorption spectra of the ring-open (A) and ring-closed (B) isomer of **2** and of Cy3 (C). Fluorescence emission spectrum of Cy3 when excited at 510 nm (D).

excellent water-solubility and relatively narrow size distribution as confirmed by transmission electron microscopy and dynamic light scattering (see Figure S10 and Table S2 in the Supporting Information).

The photoswitching experiment was performed using aqueous solutions in cuvettes monitoring with UV/Vis and fluorescence spectroscopy (Figure 1 and Figures S13–S20 in the Supporting Information). In fact, deionized water is inappropriate as medium for biological systems (cells and animals), thus we prepared sample solutions in phosphate-buffered saline (PBS; higher in ionic strength) as well as in deionized water. A 590 nm light, which coincided with the absorption maximum of the ring-closed isomer of **2** and did not overlap with the absorption band of Cy3 (i.e., no photobleaching), was used for the visible-light source (Scheme 1c). As a control, the aqueous solution of diarylethene **2** or Cy3 was first exposed to alternate irradiation with UV (365 nm, 2 min) and visible (590 nm, 30 min) light. Interestingly, the concentration of the ring-closed isomer of **2** after irradiation with UV light was slightly higher in PBS (by ca. 16%) than in deionized water (Figure S13 in the Supporting Information). In fact, the cyclization quantum yield of a diarylethene derivative was reported to be dependent on the ratio of two conformers, antiparallel and parallel, in the ring-open isomer.[10] Therefore, this suggests that for the ring-open isomer of **2**, the amount of the antiparallel conformation relative to that of the parallel conformation is higher in PBS than in deionized water. Essentially no fluorescence was detected from diarylethene **2** under the photoswitching conditions in either solution. For Cy3, no change in the absorption and emission spectra was found over three cycles of photoswitching (Figure S14 in the Supporting Information). Next, photoswitching experiments were conducted for up to five cycles using dendritic nanocluster **6** or **7** (Figure 1 and Figures S15 and S16). A small red-shift in the emission maximum of Cy3 (562.5 nm as a free dye) was noticed when conjugated to the nanocluster (566.0 nm). All sample solutions of nanoclusters showed reversible fluorescence quenching, with **7** prepared in PBS being the most efficient (47% reduction in fluorescence intensity; Table S3 in the Supporting Information). The degree of fluorescence quenching was roughly correlated to the amount of available ring-closed isomer of diarylethene relative to that of Cy3 ($A_{589,\text{after UV}}/A_{\text{Cy3 max, after Vis}}$). Taken together, the relative availability of the ring-closed isomer was higher for the neutral nanocluster **7** compared with the anionic nanocluster **6** in either solution, and the fluorescence quenching was more effective if photoswitching was performed in PBS, particularly for **7** (Fig-

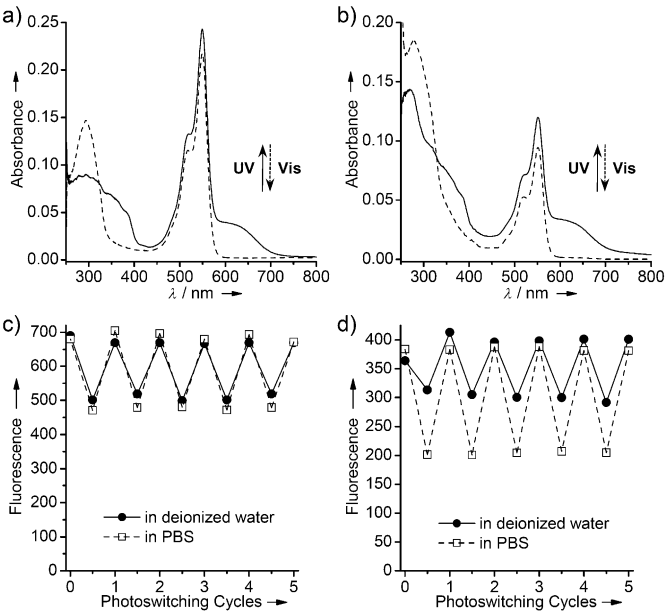

Figure 1. Reversible photoswitching experiments using dendritic nanoclusters **6** (a, c) and **7** (b, d) in aqueous solutions (100 μg mL^{-1}): a, b) UV/Vis spectra in PBS (pH 7.4); c, d) fluorescence intensity measured at 566 nm (irradiation at 510 nm). Photoswitching was repeated for up to five cycles, and the samples were irradiated alternately with UV (365 nm, 2 min, 2.60 mW cm^{-2}) and visible (590 nm, 30 min, 250–255 mW) light, beginning with UV light. For UV/Vis spectra, the average intensity values at each data point of the first five cycles were plotted.

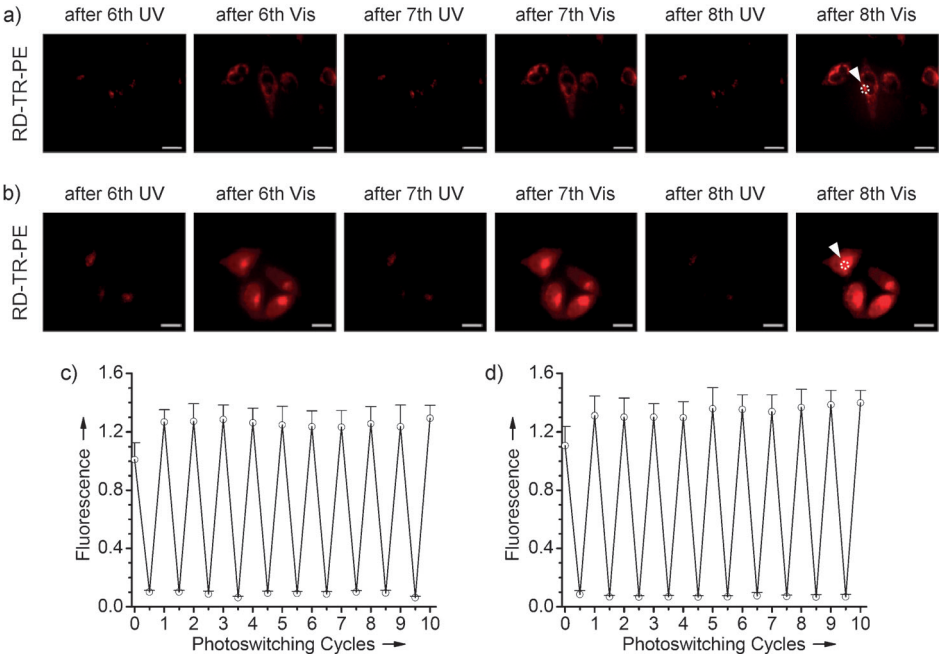

Figure 2. Photoswitching experiments performed on living HeLa cells with internalized dendritic nanoclusters **6** (a, c) or **7** (b, d). Cells were irradiated alternately with UV (365 nm, 2 min) and visible (590 nm, 30 min) light for up to 10 cycles. a, b) Fluorescence microscopy images of living HeLa cells. c, d) The average fluorescence intensity values (mean ± standard deviation (SD)) measured at the region of interest (ROI; dotted circles, 49 data points each) after each light application are plotted. Sequential irradiation with UV (loss of fluorescence) and visible (fluorescence recovery) light constitutes one full cycle of photoswitching (integers on the x-axis). RD-TR-PE: red fluorescence. Scale bars, 20 μm.

ure 1 d), than if the photoswitching was performed in deionized water.

Next, the photoswitching experiment was conducted using living HeLa (human epithelial cervical cancer) cell cultures[11] with internalized nanoclusters under the same conditions as for the solution samples (Figure 2 and Figure S24 and Table S3 in the Supporting Information). The optimal concentration of nanoclusters (10 μg mL^{-1}) and incubation time (30 min at 37 °C) were determined based on the cytotoxicity profile (Figure S21 in the Supporting Information) and kinetics of cellular uptake (Figures S22 and S23 in the Supporting Information).[12] Overall, nanocluster **7** showed higher cell viability and superior uptake efficiency[13] compared with **6**. Interestingly, both nanoclusters taken up by living cells exhibited higher on–off contrast when photoswitched (14.2 for **6** and 19.1 for **7**; Figure 2 c, d) compared with that measured in a cuvette (1.3–1.9; Figure 1 c, d and Table S3). This is probably due to the distinct physicochemical properties (pH value, temperature, salts, etc.) in the intracellular microenvironment of living cells compared with those of the bulk solutions. Moreover, no apparent change in the cellular morphology (i.e., no damage) was noticed during the photoswitching experiments that were repeated for up to 10 cycles.

A recent report described photoswitching inside a living worm by the internalized diarylethene that regulated its movement.[14] Herein, a zebrafish (*Danio rerio*)[15] was chosen as an in vivo model to evaluate the feasibility of reversible fluorescence switching by the internalized dendritic nanoclusters. Despite the wide utility of zebrafish in biomedical research, only a few reported studies have employed fluorescent probes based on nanomaterials for zebrafish imaging.[15d] Dendritic nanocluster **7** was used for its uptake, presumably by a cutaneous route,[15c] by a three-day-old zebrafish. Remarkably strong Cy3 fluorescence was observed from the zebrafish incubated with **7**. Furthermore, a successful reversible photoswitching for up to 10 cycles was achieved from living zebrafish treated with **7** (Figure 3 a, c) without any noticeable morphological defects.[15b] Indeed, the photoswitching of fluorescence was enabled by the internalized dendritic nanocluster as confirmed by cryo-sectioning (Figures S26 and S27 in the Supporting Information).

Herein, the internalization of **7** into zebrafish by permeation, however, did not lead to fluorescence inside the blood vessels. The use of reversibly photoswitchable dendritic

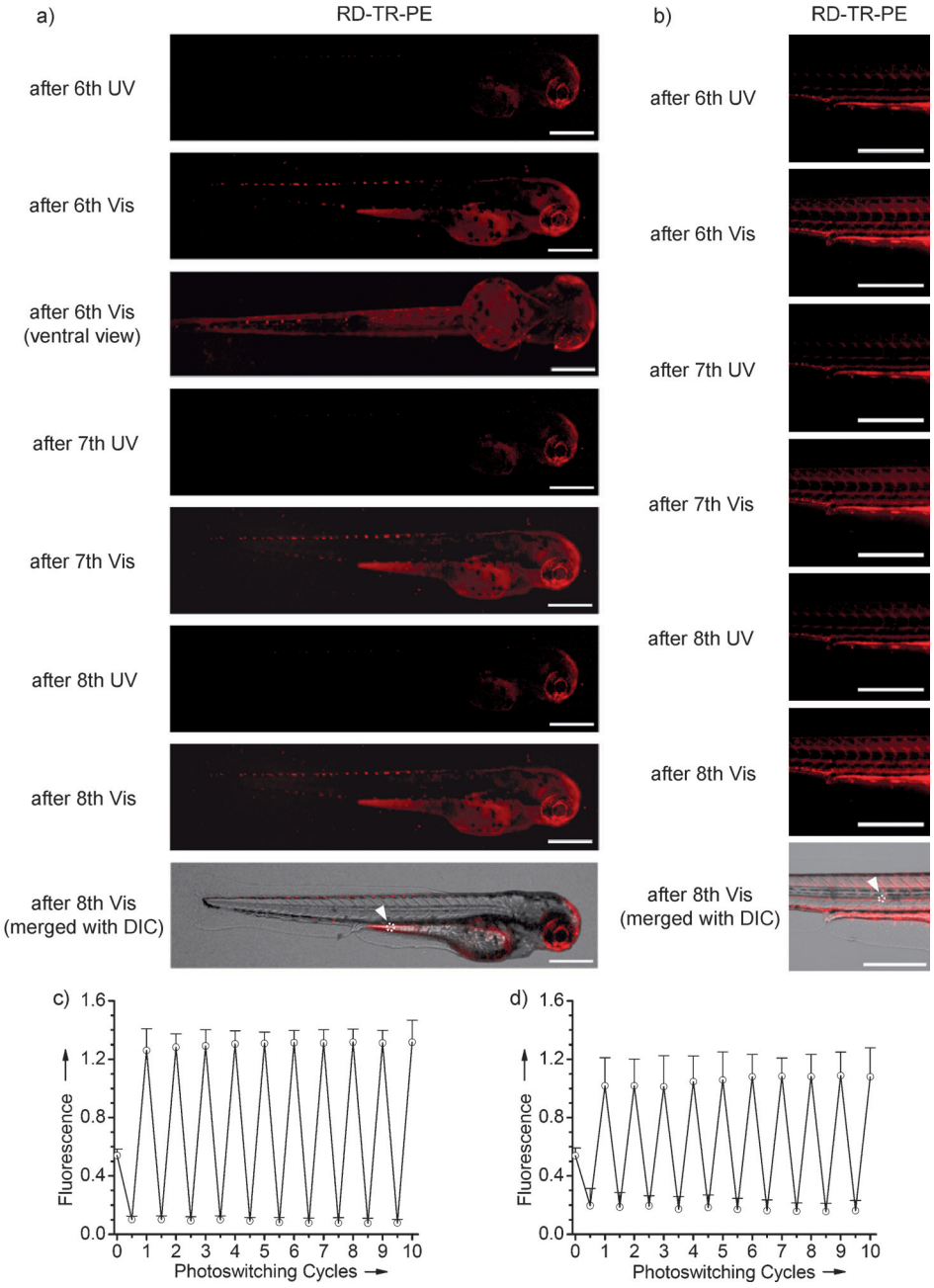

Figure 3. Photoswitching experiments performed on living zebrafish with dendritic nanoclusters **7** internalized by a, c) permeation or b, d) microinjection. The zebrafish was irradiated alternately with UV (365 nm, 2 min) and visible (590 nm, 30 min) light for up to 10 cycles. a, b) Fluorescence microscopy images of living zebrafish. c, d) The average fluorescence intensity values (mean ± SD) measured at the ROI (dotted circles, 49 data points each) after each light application are plotted. Sequential irradiation with UV (loss of fluorescence) and visible (fluorescence recovery) light constitutes one full cycle of photoswitching (integers on the *x*-axis). DIC: differential interference contrast; RD-TR-PE: red fluorescence. Scale bars, 400 μm.

nanoclusters for fluorescence imaging of the intravascular region may aid in the facile detection of many crucial diseases such as inflammation, arthritis, cancer, and cardiovascular disease. Accordingly, microinjection[16] of **7** into a two-day-old zebrafish was carried out to test the feasibility of photoswitching inside the blood vessels.[17] The Cy3 fluorescence was clearly observed from the blood vessels of a living zebrafish. Subsequently, the photoswitching of nanocluster **7** inside the vascular system of a zebrafish was performed five days post fertilization (dpf), when the formation of blood vessels in zebrafish was nearly complete. To determine the photoswitching efficiency, the lateral region of a zebrafish, where the tissue layers are shallow enough to visualize the individual blood vessels, was selected for analysis. Although slightly less on–off contrast was achieved compared with the incubation method (6.0 by microinjection vs. 14.8 by permeation; Table S3 in the Supporting Information), the reversible photoswitching of **7** inside the blood vessels of a living vertebrate was fulfilled successfully (Figure 3b,d) without any apparent harmful effects (Figure S28 in the Supporting Information).

In summary, reversibly photoswitchable dendritic nanoclusters for fluorescence imaging in vivo were developed using the diarylethene derivative **2** as a crosslinker, which showed high on–off contrast (6.0–19.1) in living systems. Moreover, to our knowledge, this is the first biocompatible fluorescent nanostructure that has internalized effectively into a living zebrafish via two independent routes—permeation and microinjection—for the imaging of interior organs and blood vessels, respectively. Unlike the recently reported photoswitchable GFP-like proteins,[18] our biocompatible dendritic nanoclusters for high-contrast reversible photoswitching do not require complex biological manipulations such as genetic encoding and protein expression and can be simply treated to or injected into living cells and organisms like small-molecule fluorophores without any noticeable toxicity or immunogenic concerns. Additional functional units such as targeting groups can be attached to the surface of these nanoclusters to accomplish multiple goals simultaneously. Furthermore, with proper structural modification of the diarylethene component, the spectroscopic properties can be tuned for photoswitching at a desired wavelength. We envision that our water-soluble and relatively nontoxic dendritic nanoclusters may facilitate fluorescence imaging in vivo by enhancing its resolution through the reversibly controlled exhibition of high on–off contrast.

Received: October 6, 2011
Revised: December 12, 2011
Published online: February 3, 2012

Keywords: dendrimers · fluorescence · FRET · photoswitch · zebrafish

[1] a) H. Kobayashi, M. Ogawa, R. Alford, P. L. Choyke, Y. Urano, *Chem. Rev.* **2010**, *110*, 2620–2640; b) V. Ntziachristos, *Annu. Rev. Biomed. Eng.* **2006**, *8*, 1–33.

[2] a) H. Kobayashi, P. L. Choyke, *Acc. Chem. Res.* **2011**, *44*, 83–90; b) R. Weissleder, C.-H. Tung, U. Mahmood, A. Bogdanov, Jr., *Nat. Biotechnol.* **1999**, *17*, 375–378.

[3] a) M. Irie, *Chem. Rev.* **2000**, *100*, 1685–1716; b) C. Yun, J. You, J. Kim, J. Huh, E. Kim, *J. Photochem. Photobiol. C* **2009**, *10*, 111–129.

[4] T. Sakata, Y. Yan, G. Marriott, *Proc. Natl. Acad. Sci. USA* **2005**, *102*, 4759–4764.

[5] a) M. Irie, T. Fukaminato, T. Sasaki, N. Tamai, T. Kawai, *Nature* **2002**, *420*, 759–760; b) L. Giordano, T. M. Jovin, M. Irie, E. A. Jares-Erijman, *J. Am. Chem. Soc.* **2002**, *124*, 7481–7489; c) M. Sauer, *Proc. Natl. Acad. Sci. USA* **2005**, *102*, 9433–9434; d) N. Soh, K. Yoshida, H. Nakajima, K. Nakano, T. Imato, T. Fukaminato, M. Irie, *Chem. Commun.* **2007**, 5206–5208; e) J. Cusido, E. Deniz, F. M. Raymo, *Eur. J. Org. Chem.* **2009**, 2031–2045; f) S. A. Díaz, G. O. Menéndez, M. H. Etchehon, L. Giordano, T. M. Jovin, E. A. Jares-Erijman, *ACS Nano* **2011**, *5*, 2795–2805.

[6] R. Esfand, D. A. Tomalia, *Drug Discovery Today* **2001**, *6*, 427–436.

[7] a) P. K. Maiti, T. Çağin, G. Wang, W. A. Goddard III, *Macromolecules* **2004**, *37*, 6236–6254; b) H. Lee, J. R. Baker, Jr., R. G. Larson, *J. Phys. Chem. B* **2006**, *110*, 4014–4019; c) C. L. Jackson, H. D. Chanzy, F. P. Booy, B. J. Drake, D. A. Tomalia, B. J. Bauer, E. J. Amis, *Macromolecules* **1998**, *31*, 6259–6265.

[8] a) Z. Cheng, D. L. J. Thorek, A. Tsourkas, *Angew. Chem.* **2010**, *122*, 356–360; *Angew. Chem. Int. Ed.* **2010**, *49*, 346–350; b) Y. Kim, M. F. Mayer, S. C. Zimmerman, *Angew. Chem.* **2003**, *115*, 1153–1158; *Angew. Chem. Int. Ed.* **2003**, *42*, 1121–1126.

[9] T. Hirose, K. Matsuda, M. Irie, *J. Org. Chem.* **2006**, *71*, 7499–7508.

[10] S. Kobatake, T. Yamada, K. Uchida, N. Kato, M. Irie, *J. Am. Chem. Soc.* **1999**, *121*, 2380–2386.

[11] Y. Zou, T. Yi, S. Xiao, F. Li, C. Li, X. Gao, J. Wu, M. Yu, C. Huang, *J. Am. Chem. Soc.* **2008**, *130*, 15750–15751.

[12] O. P. Perumal, R. Inapagolla, S. Kannan, R. M. Kannan, *Biomaterials* **2008**, *29*, 3469–3476.

[13] Our preliminary investigation suggested that several cellular uptake pathways are simultaneously involved in the internalization of both nanoclusters, with macropinocytosis being the most preferred route. Macropinocytosis is known to allow for the increased uptake and facile release of macromolecules into the cytosol while avoiding lysosomal degradation (see Figure S25 in the Supporting Information): I. A. Khalil, K. Kogure, H. Akita, H. Harashima, *Pharmacol. Rev.* **2006**, *58*, 32–45.

[14] U. Al-Atar, R. Fernandes, B. Johnsen, D. Baillie, N. R. Branda, *J. Am. Chem. Soc.* **2009**, *131*, 15966–15967.

[15] a) S.-K. Ko, X. Chen, J. Yoon, I. Shin, *Chem. Soc. Rev.* **2011**, *40*, 2120–2130; b) V. E. Fako, D. Y. Furgeson, *Adv. Drug Delivery Rev.* **2009**, *61*, 478–486; c) S. Harper, C. Usenko, J. E. Hutchison, B. L. S. Maddux, R. L. Tanguay, *J. Exp. Nanosci.* **2008**, *3*, 195–206; d) S. Rieger, R. P. Kulkarni, D. Darcy, S. E. Fraser, R. W. Köster, *Dev. Dyn.* **2005**, *234*, 670–681; e) C. Nüsslein-Volhard, R. Dahm, *Zebrafish*, Oxford Univ. Press, Oxford, **2002**.

[16] B. M. Weinstein, D. L. Stemple, W. Driever, M. C. Fishman, *Nat. Med.* **1995**, *1*, 1143–1147.

[17] A. A. Beharry, L. Wong, V. Trepepe, G. A. Woolley, *Angew. Chem.* **2011**, *123*, 1361–1363; *Angew. Chem. Int. Ed.* **2011**, *50*, 1325–1327.

[18] a) T. Grotjohann, I. Testa, M. Leutenegger, H. Bock, N. T. Urban, F. Lavoie-Cardinal, K. I. Willig, C. Eggeling, S. Jakobs, S. W. Hell, *Nature* **2011**, *478*, 204–208; b) T. Brakemann, A. C. Stiel, G. Weber, M. Andersen, I. Testa, T. Grotjohann, M. Leutenegger, U. Plessmann, H. Urlaub, C. Eggeling, M. C. Wahl, S. W. Hell, S. Jakobs, *Nat. Biotechnol.* **2011**, *29*, 942–947.

